

INVITED PAPER

PACS numbers: 42.65.An; 42.70.Qs; 42.25.Fx
DOI: 10.1070/QE2004v034n07ABEH002810

Diagnostics of the inhomogeneous distribution of quadratic optical susceptibility over parametric scattering spectra

G.Kh. Kitaeva, A.N. Penin

***Abstract*. A new method is proposed for measuring the spatial distribution of the quadratic susceptibility of inhomogeneous nonlinear media. The method is based on the unique relation of the Fourier harmonics of this distribution with the shape of a signal-radiation line during parametric frequency conversion in a linear regime. The diagnostic possibilities of the method of spontaneous parametric scattering of light are analysed by simulating the spectra of nonlinear diffraction in layered structures with different profiles of variation in the quadratic susceptibility. The cases of step and smoothed variations in the susceptibility of periodically poled regular and irregular superlattices (structures formed by the layers of optically linear and nonlinear media) are considered and the effect of light absorption at an idler frequency is studied. The experimental spectra of periodically poled crystals are presented. Different methods for measuring the one-dimensional dependence of quadratic susceptibility on the coordinate in periodically poled structures and polydomain crystals are proposed.**

Keywords: *quasi-phase matching, periodically poled structure, parametric scattering, quadratic susceptibility, spatial Fourier harmonics.*

1. Introduction

Nonlinear-optical processes in media with periodically spatially modulated optical parameters have aroused considerable recent interest. Nonlinear media with the periodically modulated quadratic susceptibility, including periodically poled crystals (PPCs), are widely used for efficient frequency conversion of optical radiation (frequency doubling, summation, subtraction, and higher-order frequency generation [1 – 8]) in various schemes of cascade interactions [9 – 11], parametric decay [12 – 14], etc. The inhomogeneous distribution of susceptibility in such structures gives rise to new conditions for the efficient frequency conversion, which are related to the so-called quasi-phase matching. In the case of quasi-phase matching, the nonzero phase mismatch of the waves involved in frequency conversion (which is, as a rule, caused by the insufficient birefringence of a homogeneous medium) is compensated due to the vectors of a reciprocal superlattice, which characterises the inhomogeneous distribution of the susceptibility. Media with the periodically spatially modulated linear susceptibility can form structures with forbidden photonic bands (photonic crystals) [15]. Apart from other various applications [15 – 17], these media can be quite promising for frequency conversion [18 – 22]. A highly efficient frequency conversion is achieved in such media both due to quasi-phase matching and an increase in the density of states of the field when the frequencies of the interacting waves approach the boundaries of forbidden bands.

The study of nonlinear optical processes in spatially irregular structures is of interest in itself. Certain types of quasi-regular structures are used for the efficient frequency conversion of broadband radiation [23]. Parametric processes in irregular media can be used for diagnostics of layered solid-state structures, domain systems, inhomogeneous twin crystals, growth inhomogeneities, etc. [24, 25]. A separate scope of problems appears in the study of the field-quadratic response of the structures consisting of alternating centrally symmetric materials with zero macroscopic quadratic susceptibilities.

The idea of using quasi-phase matching in parametric interactions in regular structures was first proposed by Bloembergen already at the very beginning of the nonlinear optics era [26]. Quasi-synchronous structures were obtained in the first experiments by simply assembling a sequence of thin crystal plates with differently oriented crystallographic axes, similarly to the Scholtz filter in linear optics.

An alternative converter element consisting of macroscopic layers made of different materials is polydomain crystals. The idea of their using was put forward already at the first stages of the development of quasi-phase-matched frequency conversion [27, 28]. The first experiment on quasi-phase-matched frequency conversion in a polydomain ferroelectric crystal was probably reported in 1964 [29]. However, to achieve the maximum conversion efficiency in polydomain crystals, layered domain structures with identically oriented domain walls and a high degree of regularity of alternating domains of specified sizes should be prepared.

Various methods for manufacturing such structures were proposed in the 1980s and were actively developed in the 1990s [1, 30]. At present a $LiNbO_3$ crystal, doped, as a rule, with antiphotorefractive impurities (Mg, Sc, Y, etc.) to increase its radiation resistance, has become an absolute

G.Kh. Kitaeva, A.N. Penin Department of Physics, M.V. Lomonosov Moscow State University, Vorob'evy gory, 119992 Moscow, Russia; e-mail: kiy@qopt.phys.msu.ru

Received 20 January 2004; revision received 27 April 2004
Kvantovaya Elektronika **34** (7) 597 – 611 (2004)
Translated by M.N. Sapozhnikov

leader among polycrystalline media used for highly efficient parametric conversion of optical waves under quasi-phase-matching conditions [31, 32]. A regular domain structure can be produced in these crystals by changing the polarisation of single-domain samples [33 – 36] or directly during the crystal growth [37 – 40]. The transverse and longitudinal sizes of samples obtained by growth methods can achieve the sizes of conventional single-crystal frequency converters.

The polar axis in PPCs rotates by 180° upon transition from one domain to another. For the properly chosen type of three-wave interaction, this may result in a change in the sign of nonlinear polarisation of the medium at the signal-radiation frequency. In this case, the maximum modulation of the effective value of the quadratic susceptibility of the medium occurs. At the same time, the modulation of the linear susceptibility and refractive index is almost insignificant because the modulation depth is, as a rule, smaller than 0.01 % [41]. Therefore, a purely nonlinear superlattice is formed in the crystal, and the propagation of waves in the superlattice upon three-wave parametric interaction can be called nonlinear diffraction of light [28, 42]. In the case of quasi-phase matching, the maximum elements of the quadratic susceptibility tensor of the crystal are commonly used, which cannot be employed in synchronous conversion in a single-domain sample. A highly efficient transfer of the signal-radiation energy to the required diffraction order becomes possible, several three-wave processes can be simultaneously realised, and optical harmonics of different orders can be obtained in the same optical element [7, 8, 43, 44].

To provide the efficient frequency conversion, it is necessary to use bulk layered structures, which have certain properties, namely, plane and strictly regularly arranged layers ensuring the reproducibility of the superlattice constant with a high precision. In some cases (especially, when several orders of nonlinear diffraction are used at once), the requirements are imposed directly on the profile of the quadratic susceptibility distribution with one period of a nonlinear superlattice. When quasi-regular structures (for example, nonlinear Fibonacci lattices [23]) are used, a certain law of variation in the quadratic susceptibility along the specified direction must be fulfilled.

The problems of the development of methods for controlling the quality of nonlinear optical superlattices (both integral and differential) and determining all the details of a variation in the quadratic susceptibility within the active volume of a nonlinear element become increasingly urgent. The use of conventional methods for this purpose, which are based on chemical etching of surfaces (followed by atomic-force microscope imaging, the profilometer study of surfaces, etc. [45]), X-ray analysis of the volume structure of crystals [38], and the study of the electro-optical response, is obviously insufficient, and optical methods to control the entire active volume of a nonlinear element are required. Because we are dealing with the study of a nonlinear superlattice, a method based on parametric interactions is needed. These problems can be partially solved by using methods based on a comparison of the intensities of the second-harmonic radiation emitted from different sites of a crystal. Signals from different sites of a crystal are separated either by irradiating only these sites [46] or by imaging luminous layers in the second-harmonic field [24, 25]. The second method, which is called a second-harmonic microscope, can be used to analyse domain structures only in the case of interference of signals from a regular domain structure and from homogeneous samples [24]. It seems that a method based on spontaneous parametric scattering (SPS) of light can become one of the simplest and efficient methods for diagnostics of variations in the optical quadratic susceptibility within the entire volume of a crystal.

SPR is a spontaneous decay of monochromatic (pump) photons into pairs of lower-frequency photons consisting of the 'signal' photons, i.e., output photons detected at the exit from a medium, and the 'idler' photons conjugated with signal photons. In principle, idler and signal photons in SPS are equivalent, and both of them can be detected. The decay occurs in a medium without the symmetry centre, which has the quadratic susceptibility [47]. As a result, broadband output radiation is emitted from the medium. The only requirement imposed under stationary conditions on the frequencies of photons created in scattering is the equality of their sum to the pump frequency. At present, SPS is widely used to prepare biphotonic states in modern quantum optics [48 – 50] and for measuring optical and dynamical parameters of phonon polaritons in spectroscopy [51 – 54]. The SPR method is also promising for the absolute calibration of the brightness of radiation sources and the quantum efficiency of photodetectors in quantum photometry [55 – 59].

The aim of this paper is to study SPS in crystals with a spatially inhomogeneous distribution of the quadratic susceptibility, to investigate the properties of two-dimensional frequency-angular SPS spectra related to the spatial inhomogeneity and structure of the superlattice, and to analyse thereby the diagnostic possibilities of the SPS method for solving the inverse problem of determining the spatial distribution of the quadratic susceptibility in crystals with nonlinear superlattices. We consider here not only regular inhomogeneities in layered polydomain crystals (one-dimensional nonlinear superlattices) but also inhomogeneities with a variable period, different numbers of layers, and with possible absorption at the idler radiation frequency. In addition, we considered the properties of SPS in structures consisting of rather thin, but macroscopic (1 – 100 μm) layers with nonlinear optical properties separated by layers of an optically linear medium.

2. The SPS line shape in media with nonlinear superlattices

The SPS line shape in a transparent medium with an arbitrary spatial distribution of the quadratic susceptibility can be analysed directly within the framework of the perturbation quantum theory. This method has already been used for a particular case of nonlinear interference in layers with alternating values of the quadratic susceptibility [60 – 64]. If absorption of idler waves should be taken into account, the nonlinear fluctuation-dissipative theorem can be used [47], as was done in Ref. [64] to take into account absorption in nonlinear interferometers, or the method of generalised Kirchhoff's law (GKL), which was developed by Klyshko [47, 65] for a unified description of spontaneous and stimulated three-wave parametric processes in dissipative media. The GKL method makes it possible to determine the second correlation moments of fields at the output of a nonlinear medium from second correlation moments specified at the input. In this case, a linear relation

between the Heisenberg operators of the input and output fields is postulated in terms of the scattering matrix.

In Ref. [66], general relations are presented, which were obtained by the GKL method and relate the SPS line shape to the Fourier harmonics of an arbitrary spatial distribution of the quadratic susceptibility in a nonlinear absorbing medium. In the case of absorption of idler waves, the expression for the differential power of the SPS signal radiation per unit angular and spectral intervals has the form

$$P_{\omega_1\Omega_1} = C_0 \sum_{m=-\infty}^{\infty} |\chi_m|^2 g(\Delta_m, y_2) + C_0 \sum_{m=-\infty}^{\infty} \sum_{\substack{m'=-\infty \\ m' \neq m}}^{\infty} (-1)^{n(m'-m)} \chi_m^* \chi_{m'} \times \left[\frac{\exp(-\mathrm{i}\Delta - y_2) - 1}{(y_2 + \mathrm{i}\Delta - \mathrm{i}2\pi mn)(y_2 + \mathrm{i}\Delta - \mathrm{i}2\pi m'n)} + \frac{\exp(\mathrm{i}\Delta - y_2) - 1}{(y_2 - \mathrm{i}\Delta - \mathrm{i}2\pi mn)(y_2 - \mathrm{i}\Delta - \mathrm{i}2\pi m'n)} \right], \quad (1)$$

where $g(\Delta_m, y_2)$ is the form factor; χ_m are the amplitudes of spatial harmonics of the Fourier spectrum of the spatial distribution of the quadratic susceptibility $\chi^{(2)}(z)$ of the medium:

$$\chi^{(2)}(z) = \sum_{m=-\infty}^{\infty} \chi_m \exp(\mathrm{i}mqz), \qquad \chi_m = \frac{1}{d} \int_{-d/2}^{d/2} \chi^{(2)}(z) \exp(-\mathrm{i}mqz) \mathrm{d}z; \quad (2)$$

d is the period of a one-dimensional nonlinear superlattice in the case of a regular distribution of $\chi^{(2)}(z)$ or a total length l of the medium along the direction z in the case of an irregular distribution; $n = l/d$ is the number of periods d fitting a total length l [a sample of length l with an irregular dependence $\chi^{(2)}(z)$ can be treated as a part of an in finite regular lattice with the period $d = l$; therefore, the function $\chi^{(2)}(z)$ can be expanded on a finite interval from $-l/2$ to $+l/2$ in a Fourier series]; $q \equiv 2\pi/d$ is the modulus of the reciprocal superlattice vector directed along the z axis; $k_i = \omega_i n_i/c$ are the moduli of the wave vectors of the pump ($i = 0$), signal ($i = 1$) and idler ($i = 2$) waves; ω_i are frequencies; n_i are the refractive indices of the medium at frequencies ω_i; $\Delta \equiv l(k_{1z} + k_{2z} - k_{0z})$ is the projection of the dimensionless phase mismatch on the z axis; $\Delta_m \equiv \Delta - 2\pi mn$ is the so-called quasi-phase mismatch; $C_0 \equiv [\hbar\omega_1^4\omega_2/(c^5 n_0 n_1 n_2)]P_0 l^2/\cos\vartheta_2$ is a general factor proportional to the pump power P_0; $y_2 \equiv \alpha_2 l/(2\cos\vartheta_2)$; α_2 is the absorption coefficient of the medium at the idler wave frequency; ϑ_1 and ϑ_2 are the angles between the normal to the layer boundaries and the wave vectors of the signal and idler waves inside a crystal, which are related to the corresponding angles θ_1 and θ_2 outside the crystal by Snell's law $\sin\theta_i = n_i \sin\vartheta_i$.

Relation (1) describes the signal line shape, i.e., the dependence of the differential power on the deviation from phase matching. According to (1), the SPS line shape is determined by two terms. The first one is the additive sum of contributions from individual harmonics. Each of the terms entering this sum is characterised by the same distribution of the signal intensity with respect to the quasi-phase-matching maximum ($\Delta_m = 0$) as upon scattering in a homogeneous medium with respect to the phase-matching maximum ($\Delta = 0$). However, the positions of new maxima (tuning curves for each of the terms) are shifted in the frequency–wave vector coordinate plane according to the quasi-phase-matching conditions $\Delta(\omega_1, \vartheta_1) = mql$. Each of the terms of the first sum is proportional to the square of modulus of the amplitude of the corresponding harmonic. The second term in (1) contains the products of non-coinciding harmonics χ_m and is the result of their interference.

The expression for the form factor $g(\Delta, y_2)$

$$g(\Delta, y_2) \equiv \frac{2}{(\Delta^2 + y_2^2)^2} \left[\left(\Delta^2 - y_2^2\right)\left(1 - \mathrm{e}^{-y_2}\cos\Delta\right) - 2y_2\Delta \mathrm{e}^{-y_2}\sin\Delta + y_2\left(\Delta^2 + y_2^2\right) \right], \quad (3)$$

which describes the SPS line shape in a layer, was derived in [67]. Later, the effect of reflection of the waves from the layer boundaries was considered in [68]. This effect produces additional modulation of the scattering intensity due to linear and nonlinear interference of the reflected waves. Expression (1) was derived in Ref. [66] by neglecting the reflection of light from input faces of a spatially inhomogeneous nonlinear medium and inside it because the modulation of linear optical parameters was assumed negligible. Such an approximation is justified for 'naturally inhomogeneous' structures containing domains, twins, and growth inhomogeneities due to which crystals cannot be integral structures at large gradients of linear parameters. The expression for $g(\Delta_m, y_2)$ entering the first sum in (1) is described by the same relation (3), but with the replacement $\Delta \to \Delta_m$.

When absorption of light in a medium can be neglected, relation (1) for the SPS line shape takes a simple form

$$P_{\omega_1\Omega_1} = C_0 \left| \sum_{m=-\infty}^{\infty} \chi_m \mathrm{sinc}(\Delta_m/2) \right|^2. \quad (4)$$

A similar expression describes the frequency–angular distribution of the square of modulus of the envelope of a two-photon wave packet (biphoton 'amplitude') and a change in the correlation of readings of the detectors of idler and signal radiations depending on the wave detuning. Note that the same expression, but taking into account an additional factor related to the distribution of the brightness of the external idler frequency signal, is also valid for the line shape of any three-wave parametric process in a transparent nonlinear superlattice [66] (frequency doubling, generation of the sum or difference frequencies) if the small-signal gain and linear-conversion conditions are realised. The deviation Δ_m from quasi-phase matching differs in this case from Δ by the value $2\pi mn$ as well ($\Delta_m \equiv \Delta - 2\pi mn$). The type of the process should be taken into account only in determining Δ, which is specific for each type of the interaction [69, 70].

If the energy redistribution between input and output waves occurs more intensely, the regime of the specified pump and linear gain is not satisfied, and the problem of calculation of the signal parameters is substantially complicated. In this case, it is impossible to obtain simple

analytic expressions of type (4), which would describe any possible modulation profiles of the nonlinear susceptibility, and in a number of cases, which are important for engineering nonlinear optics, the corresponding highly efficient radiation converters can be calculated only numerically [5, 44].

The modulation of the linear susceptibility of a spatially inhomogeneous nonlinear medium should be taken into account in the analysis of parametric processes in 'artificial' nonlinear superlattices assembled from different materials. The simplest variant of such a one-dimensional superlattice is a sequence of plane–parallel plates, each of them being a macroscopically homogeneous element with the known linear and nonlinear susceptibilities. Structures with a periodic modulation of the linear susceptibility may have forbidden photonic bands. Nonlinear effects in photonic crystals are usually described by neglecting the spatial modulation of the nonlinear susceptibility [19, 71, 72]. However, a weak rectangular modulation of the quadratic susceptibility was considered in some papers [18, 20, 73].

It seems that the problem of accounting for arbitrary modulation of both linear and nonlinear susceptibilities has not been solved in the general case so far. By using the approach described in Ref. [60] in the SPS study in the case of nonlinear interference, we can obtain the relation

$$P_{\omega_1\Omega_1} = \frac{C_0}{l^2}\left|\sum_{j=1}^{N}\chi_j^{(2)} l_j \mathrm{sinc}(\Delta^{(j)}/2)\exp\left(-\mathrm{i}\Delta^{(j)}/2 + \right.\right.$$

$$\left.\left. + \mathrm{i}\sum_{j'=1}^{j}\Delta^{(j')}\right)\right|^2 \qquad (5)$$

for the signal line shape at the output of an arbitrary sequence of homogeneous plates. Here, j is the ordinal number of a plate; l_j is the plate thickness; $\chi_j^{(2)}$ is the effective quadratic susceptibility; $k_i^{(j)} = \omega_i n_i^{(j)}/c$ are the moduli of wave vectors of signal ($i = 1$) and idler ($i = 2$) waves, and the pump wave ($i = 0$) in the jth plate; $n_i^{(j)}$ is the refractive index of a plate; $\Delta^{(j)} \equiv l_j(k_{1z}^{(j)} + k_{2z}^{(j)} - k_{0z}^{(j)})$ is the dimensionless deviation from phase matching in each of the plates (projection on the direction perpendicular to the plates); and $l = \sum_{j=1}^{N} l_j$ is the total thickness of the stack.

Relation (5) is valid in the small-signal-gain regime for completely transparent media in the case when the reflection of the waves from plate boundaries can be neglected. If the difference between the refractive indices of plates is neglected, relation (4) follows directly from (5).

A study of the frequency–angular distribution of the signal-wave intensity in the small-signal-gain regime can be used for measuring the spatial distribution of the quadratic susceptibility in a nonlinear medium. In principle, any three-wave parametric processes can be employed for this purpose, as well as stimulated cascade four-wave [9] up- and down-frequency conversion processes. However, when stimulated processes are used, there always exists the problem of accounting for a nonuniform filling of the converter (medium under study) modes.

This problem is absent when SPS is used. The uniform filling of the input modes of the idler channel is determined by vacuum fluctuations of the field and is warranted when the scattering regime is linear in the pump intensity. In this case, the SPS method makes it possible to analyse the distribution $\chi^{(2)}(z)$ inside an object under study.

3. Examples of experimental SPS spectra

Consider some typical cases of a periodic spatial variation of $\chi^{(2)}$ in polydomain crystals with plane domains. As a rule, three regions can be distinguished in each domain: the middle one, where the value and sign of $\chi^{(2)}$ do not virtually change, and two boundary regions (domain walls), which are directly adjacent to neighbouring domains (Fig. 1). In the region of domain walls, the effective value of $\chi^{(2)}$, determining the three-wave-process intensity, undergoes drastic variations and its sign can change. In the latter case, the magnitude of $\chi^{(2)}$ can decrease to zero in the boundary region. The thickness of intermediate layers is determined by the width of the spatial-charge region near the domain wall and by the distribution of impurities and defects in the crystal. The dimension of the middle region can be small compared to the size of intermediate layers when the total thickness of domains is relatively small.

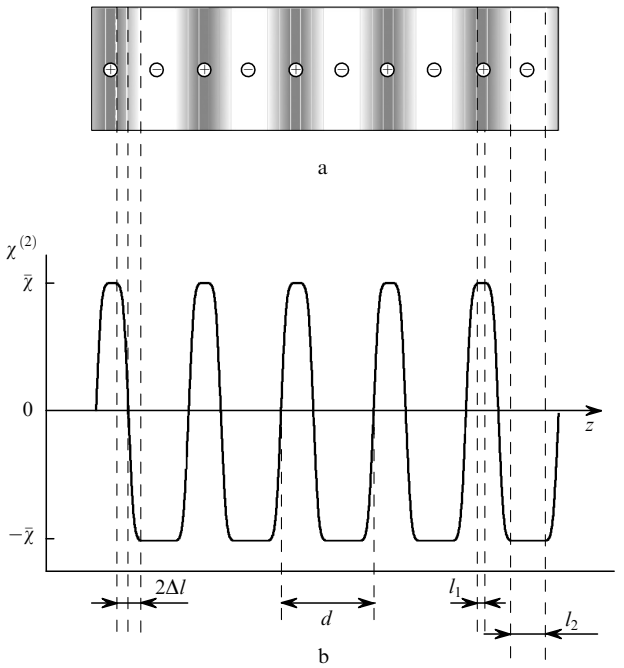

Figure 1. Schematic representation of a polydomain ferroelectric (a) (the + and − signs denote domains of opposite signs) and the dependence of the quadratic susceptibility $\chi^{(2)}$ on the displacement from one domain to another (b).

Consider in more detail two particular distributions of $\chi^{(2)}$ in polydomain structures studied in experiments on parametric scattering of light in doped lithium niobate $Nd:Mg:LiNbO_3$ and barium–sodium niobate $Ba_2NaNb_5O_{15}$ crystals with domain-structure periods of the order of 5–20 μm. The spatial modulation of $\chi^{(2)}$ (a volume nonlinear diffraction grating) in crystals was produced by growing crystals using a special procedure based on the Czochralski technique [38–40, 74–76]. The orientation of the normal with respect to domain layers in this procedure coincides with the crystal growth direction. A regular domain structure was formed in the regions of $Nd:Mg:LiNbO_3$ crystals with a layered growth inhomogeneity where the effect of the local gradient of impurity concentration during the crystal growth was stronger than that of the temperature gradient [38]. During the crystal

growth, impurities enter different sites of the crystal in a different manner, resulting in the formation of the impurity concentration gradient, which periodically changes its sign along the growth direction. When the grown crystals are cooled below the temperature of transition to the ferroelectric phase ($T_c \simeq 830-850\,^\circ$C for $Ba_2NaNb_5O_{15}$ and $1150-1180\,^\circ$C for $Nd:Mg:LiNbO_3$), a system of plane domains is formed in them, which repeat the configuration of regularly alternating growth layers.

The conditions for observing SPS in $Nd:Mg:LiNbO_3$ and $Ba_2NaNb_5O_{15}$ crystals are substantially different. The $Nd:Mg:LiNbO_3$ samples were grown along the normal to the $\{01\bar{1}2\}$ face [39, 76]. The angle between the normal to the domain surface and the second-order crystallographic axis C was 57°. This ('faced') type of the orientation provides a high optical quality of domain walls (their small thickness and the absence of curvature). The wave vector $\boldsymbol{k}_0$ of the extraordinarily polarised pump was directed during SPS perpendicular to domain layers (at an angle of 57° to the C axis). Parametric scattering as observed in the crystallographic YZ plane. The growth-layer planes in $Ba_2NaNb_5O_{15}$ samples were oriented almost perpendicular to the crystallographic C axis [74, 75]. The pump wave vector $\boldsymbol{k}_0$ was oriented during SPS virtually parallel to domain layers and perpendicular to the C axis.

Parametric scattering of light was studied using an $x-y$ SPS spectrograph [54, 77], whose optical scheme is shown in Fig. 2. Pumping was performed by cw gas He–Cd (emitting $P \approx 40$ mW at 441.6 nm) or Ar ($P \approx 500$ mW at 488.0 nm) lasers. A plane front of the pump wave was produced with the help of a long-focus lens, which compensated the angular divergence of laser radiation in a Gaussian beam waist. The required polarisation was obtained using a Glan–Thomson prism. A similar prism was placed behind the crystal to separate the required signal radiation component. Signal radiation was focused at the entrance slit of an ISP-51 spectrograph with the help of a three-lens optical system operating in the Fourier optics regime. A total filling of the spectrograph angle of view by signal radiation scattered in the angular range $\theta_1 = -12^\circ \ldots 12^\circ$ was achieved by a proper selection of the focal lengths (f_{1-3}, f'_{1-3}) and aperture ratios of lenses (or lens objectives).

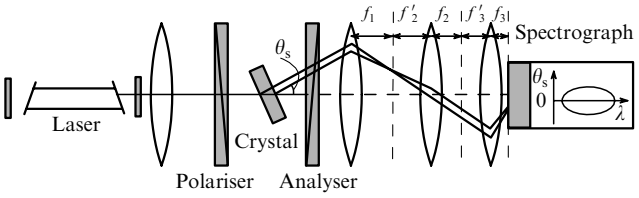

Figure 2. Optical scheme of an SPS spectrograph.

The beam displacement at the spectrograph exist slit along the spectrograph dispersion was determined by the signal radiation frequency and, hence, by the corresponding frequency of the idler radiation. A plane in which a triangle of the wave vectors of the pump, idler, and signal waves was located was specified by the entrance slit of the spectrograph. The frequency–angular intensity distribution was recorded on a photographic film. Photographic recording allowed us to obtain the SPS spectra in broad frequency and angular ranges.

3.1 SPS spectra in barium–sodium niobate crystals

Figure 3 shows a part of the scattering spectrum at the upper polariton branch for a barium–sodium niobate crystal [78, 79]. Unlike the spectrum of a homogeneous crystal, which is characterised by one closed tuning curve resembling an ellipse, the spectrum in Fig. 3 exhibits four ellipses displaced with respect to each other. The intensity of the central ellipse, which is located symmetrically with respect to the frequency axis, as in the case of a homogeneous crystal, is much lower than the intensity of two adjacent ellipses displaced upward and downward with respect to the central ellipse. The spectrum in Fig. 3 was obtained in the absence of linear diffraction of pump radiation, when the Bragg condition for a linear diffraction of the signal wave is fulfilled within a restricted part of the spectrum and explains the appearance of the fourth ellipse.

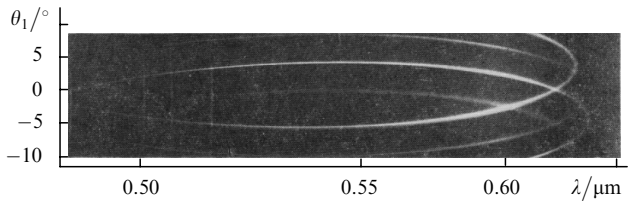

Figure 3. Region of the frequency–angular parametric scattering spectrum at the upper polariton branch in a periodically poled barium–sodium niobate crystal.

The appearance of three closed curves in the spectrum of a layered crystal is well described by the theory of nonlinear diffraction in a simplest case when the contributions from interference terms are insignificant. The refractive index n_2 of the crystal at the idler frequency, the period d of the domain structure, and the slope of the vector of domain superlattice with respect to the normal to the front face by the angle θ were calculated assuming that the observed curves are tuning curves of the zero- and ±first-order nonlinear diffraction. The measurements of θ and d at different frequencies of the signal wave gave the values $\theta = 89.3^\circ \pm 0.2^\circ$ and $d/2 = 6.05 \pm 0.05$ μm.

Figure 4 shows the dispersion of the refractive index calculated for two tuning curves for two barium–sodium niobate crystals with different domain structures. The results of these calculations well coincide with each other within the error of measurements of n_2 to the third decimal place. This proves that the observed curves do appear due to nonlinear diffraction of the corresponding orders.

The frequency–angular shape of a scattering line, the number and mutual arrangement of the displaced tuning curves forming the SPS spectrum of a periodically poled crystal allow the measurement of the spectrum of reciprocal superlattice vectors. The intensity of a signal scattered to the zero diffraction order (Fig. 3) is much lower than that for scattering to the first orders. Almost no scattering to other diffraction orders is observed. This suggests that the distribution $\chi^{(2)}(z)$ is close to the harmonic form $\chi^{(2)}(z) \approx \chi_0 + \chi_1 \cos(qz)$, with $\chi_0 < \chi_1$. The ratio χ_0/χ_1 gives information on the unipolarity of the sample region studied, i.e., on the difference between total thicknesses (or volumes) of positive and negative domains. The smaller is χ_0/χ_1, the closer is total thicknesses to each other. The absence of higher harmonics in the spectrum of $\chi^{(2)}(z)$ suggests that the thicknesses of domains and boundary regions (domain

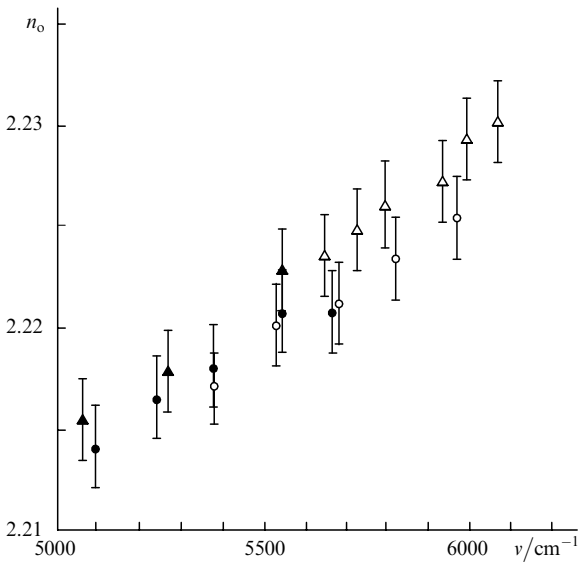

Figure 4. Dispersion of the ordinary refractive index n_o for periodically poled barium–sodium niobate crystals with different parameters (circles: the domain thickness is 6.05 ± 0.05 μm, the angle between layers and the axis C is $89.3^\circ \pm 0.2^\circ$; triangles: the domain thickness is 9.1 ± 0.05 μm and the angle is $87.7^\circ \pm 0.2^\circ$) in the IR spectral range calculated by the tuning curves of SPS in the zero (dark circles and triangles) and first (open circles and triangles) orders of nonlinear diffraction.

walls), in which the quadratic susceptibility predominantly changes, are comparable.

3.2 SPS spectra in doped lithium niobate crystals

Figure 5 demonstrates the frequency–angular SPS spectra for mono- and polydomain lithium niobate crystals [9, 80]. A comparative analysis of the spectra shows that the spectrum of a polydomain crystal exhibits additional tuning curves, which are especially distinct in the region of scattering on the upper polariton branch (in the idler frequency region $\nu_2 \geqslant 900$ cm^{-1}). The dispersion curves for the ordinary refractive index in the region of the upper polariton branch in mono- and polydomain samples, determined from the tuning curves, are shown in Fig. 6. The domain-structure period measured in experiments is $d = 5.6 \pm 0.2$ μm. We have also found that the additional tuning curve in the SPS spectrum of the polydomain sample in the region of the upper polariton branch corresponds to the spatial harmonic χ_m with the index $m = -1$.

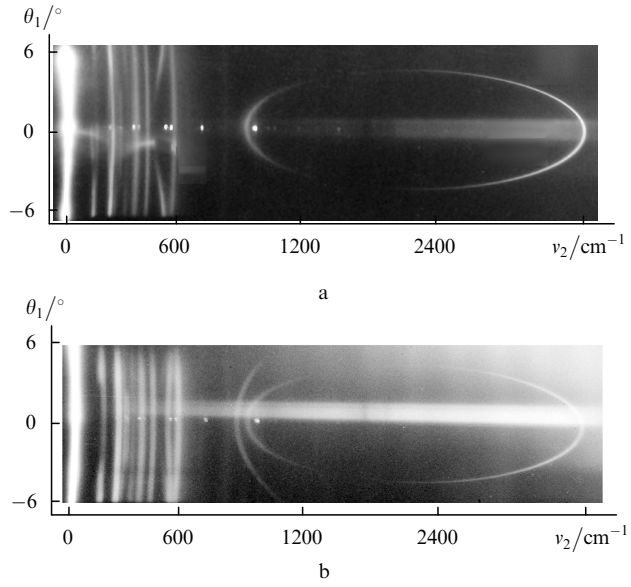

Figure 5. Frequency–angular spectra of parametric scattering of light in monodomain (a) and polydomain (b) lithium niobate crystals. The entrance and exit faces of samples are cut parallel to growth layers.

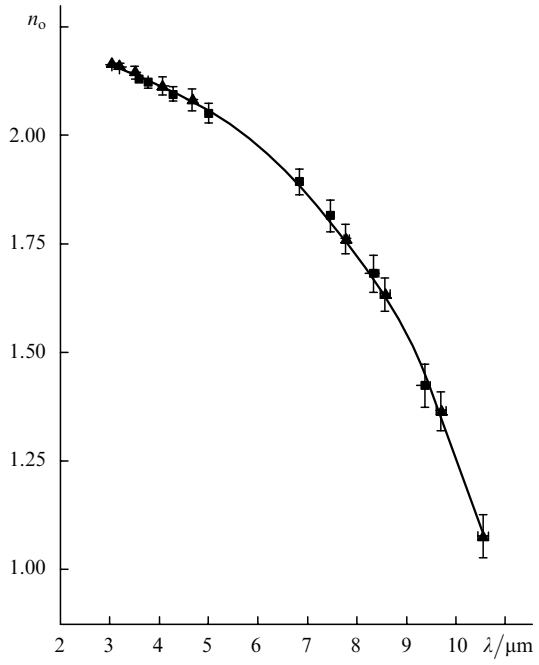

Figure 6. Dispersion of the ordinary refractive index n_o of $Nd:Mg:LiNbO_3$ crystals in the region of the upper polariton branch for a polydomain crystal with the molar concentrations of neodymium and magnesium equal to 0.33 ± 0.05 % and 2.05 ± 0.05 %, respectively (▲), and for a polydomain crystal with the molar concentrations of neodymium and magnesium equal to 0.34 ± 0.05 % and 2.56 ± 0.05% (■), respectively.

The numerical calculations of the part of the spectrum corresponding to scattering on the lower polariton branch in the vicinity of the ~580-cm^{-1} fundamental vibration of the E type showed that the distinct tuning curve corresponds to two blended curves related to the spatial harmonics χ_m with indices $m = \pm 1$. The low-intensity parts of the tuning curve corresponding to $m = 0$ are observed only in the region of large scattering angles near the photon frequency.

Similar relations between the powers of scattering into different orders of nonlinear diffraction are presented in [41] for a $Y:Mg:LiNbO_3$ crystal with a similar domain structure. No additional tuning curves corresponding to the higher orders of nonlinear diffraction were observed. This is probably explained by the fact that the amplitudes of the corresponding spatial harmonics χ_m are very small.

Note that the spectra of parametric scattering observed in the case of nonlinear diffraction when the domain layers are oriented almost along the pump wave vector $\boldsymbol{k}_0$ (Fig. 3) or almost perpendicular to it (Fig. 5b) are qualitatively different. In the first case, when $\boldsymbol{q} \perp \boldsymbol{k}_0$, the presence of harmonics in the spectrum of $\chi^{(2)}(z)$ leads to the appearance

of new tuning curves, which have the shape close to that of tuning curves in a spatially homogeneous crystal, but are shifted in the angle. In the second case, when $\boldsymbol{q}\|\boldsymbol{k}_0$, the shape of new tuning curves is different and the angular shift can be absent. The tuning curves of different orders are more often shifted by frequency, which opens up the possibility for measuring polariton parameters in spectral regions that were inaccessible for crystals without a nonlinear superlattice. The reason is that the quasi-phase-matching conditions $\Delta_m = 0$ can be fulfilled in the region where the phase-matching condition $\Delta = 0$ was not satisfied. This is illustrated by a part of the spectrum near the maximum frequency (above 880 cm^{-1}) of a longitudinal phonon for the lithium niobate crystal. By measuring the refractive index over the tuning curve of the -1st nonlinear diffraction order, we determined the polariton dispersion in the vicinity of the phonon frequency region (Fig. 6).

The SPS spectra of layered barium–sodium niobate and lithium niobate crystals show that the spectrum of $\chi^{(2)}$ in crystals with the period of a nonlinear superlattice of the order of 5–20-μm contains only the lowest harmonics. This means that the middle regions of the homogeneous distribution of $\chi^{(2)}$ in domains of such a thickness are virtually absent, while the spatial distribution of the quadratic susceptibility in intermediate regions occupying the entire thickness of the domains is well described by the sinusoidal distribution.

4. Simulation of nonlinear diffraction spectra in polydomain crystals

The study of variation in the quadratic susceptibility in the 180° domain structures allowed us to restrict substantially the consideration of the possible types of the dependence $\chi^{(2)}(z)$. In most cases, including variants of an arbitrary relation between the thicknesses of intermediate and middle layers, the dependence $\chi^{(2)}(z)$ within each of the periods $[-d/2, d/2]$ of the domain structure can be represented as

$$\chi^{(2)}(z) = \begin{cases} \bar{\chi}\sin\dfrac{\pi(z+d/2)}{2\Delta l}, & -\dfrac{d}{2} < z < -\dfrac{d}{2} + \Delta l, \\ \bar{\chi}, & -\dfrac{d}{2} + \Delta l < z < -\dfrac{d}{2} + \Delta l + l_1, \\ \bar{\chi}\sin\dfrac{\pi(z+d/2-l_1)}{2\Delta l}, & -\dfrac{d}{2} + \Delta l + l_1 < z < -\dfrac{d}{2} + 3\Delta l + l_1, \\ -\bar{\chi}, & -\dfrac{d}{2} + 3\Delta l + l_1 < z < \dfrac{d}{2} - \Delta l, \\ \bar{\chi}\sin\dfrac{\pi(z-d/2)}{2\Delta l}, & \dfrac{d}{2} - \Delta l < z < \dfrac{d}{2}, \end{cases} \quad (6)$$

where $\bar{\chi}$, $-\bar{\chi}$ and l_1, l_2 are the quadratic susceptibilities and thicknesses of the middle layers of domains of the opposite signs, respectively; Δl is the boundary region thickness; and $l_1 + l_2 + 4\Delta l$ (Fig. 1). It is obvious that this relation does not describe the cases when the absolute values of $\chi^{(2)}$ are different in domains of the opposite signs. To take this difference into account, it is sufficient to add in most cases a constant to the right-hand sides of (6).

The spectrum of spatial Fourier harmonics for the periodic dependence (6) has the form

$$\chi_m = \frac{\bar{\chi}(-1)^{mn}}{\pi m}\left\{(-1)^m \sin(m\pi\rho) + \mathrm{i}\left[(-1)^m \cos(m\pi\rho) - 1\right]\right\} \times \frac{\cos(m\pi\delta)}{1 - (2m\delta)^2}. \quad (7)$$

The parameter $\rho \equiv (l_1 - l_2)/d$ characterises the difference in the thickness of homogeneous regions of domains, and the parameter $\delta \equiv 2\Delta l/d$ determines the thickness of inhomogeneous intermediate layers localised near the domain walls. Expansion (7) is possible when $d/(4\Delta l) \equiv 1/(2\delta)$ is not an integer. By substituting the amplitudes of spatial harmonics (7) into expression (4) for the signal radiation intensity in a transparent crystal, we obtain the dependence of the differential scattered power on the wave detuning in a sample containing n domain periods

$$P_{\omega_1\Omega_1} = 4C_0\bar{\chi}^2 \sin^2(\Delta/2)\left\{\left[\sum_{m=-\infty}^{\infty} \frac{(-1)^m \sin(\pi m\rho)}{\pi m(\Delta - 2\pi mn)} D_m(\delta)\right]^2 + \left[\sum_{m=-\infty}^{\infty} \frac{1 - (-1)^m \cos(\pi m\rho)}{\pi m(\Delta - 2\pi mn)} D_m(\delta)\right]^2\right\}, \quad (8)$$

where

$$D_m(\delta) \equiv \frac{\cos(\pi m\rho)}{1 - (2m\delta)^2}$$

is the factor taking into account the presence of intermediate layers at the boundaries of each of the domains. If the widths of intermediate layers are negligibly small, $\delta = 0$ and $D_m(\delta) = 1$, then the spatial distribution of the nonlinear susceptibility has the form of a meander, and the shape of the signal radiation line is described by the expression

$$P_{\omega_1\Omega_1} = C_0\bar{\chi}^2 \frac{\mathrm{sinc}^2(\Delta/2)}{\sin^2(\Delta/2n)}\left(1 - 2\cos\frac{\rho\Delta}{2n}\cos\frac{\Delta}{2n} + \cos^2\frac{\Delta}{2n}\right). \quad (9)$$

If the thicknesses of domains of the opposite signs coincide ($\rho = 0$), while intermediate layers are virtually absent ($\delta = 0$), scattering occurs only into the odd orders of nonlinear diffraction. The so-called unshifted tuning curve, which is observed during scattering in homogeneous samples with the same values of linear optical parameters, also disappears. In this case, the shape of the signal line is

$$P_{\omega_1\Omega_1} = C_0\bar{\chi}^2 \mathrm{sinc}^2(\Delta/2)\tan^2\frac{\Delta}{4n}. \quad (10)$$

This case is illustrated by the curve calculated for $n = 10$ (Fig. 7a). One can see that the maxima of nonlinear diffraction to the ± 1st orders are much more intense than other maxima. The intensity of the maxima decreases with increasing diffraction order. The consideration of the intermediate layers, which smooth off a sharp change in $\chi^{(2)}$ at the domain boundaries, leads to the intensity redistribution between the diffraction maxima of different orders, resulting in the enhancement of the first and weakening of the highest diffraction orders with increasing the relative thickness of the intermediate layer. Figure 7b shows the dependence of the differential power of signal radiation on the wave detuning in the presence of intermediate layers occupying about half each period

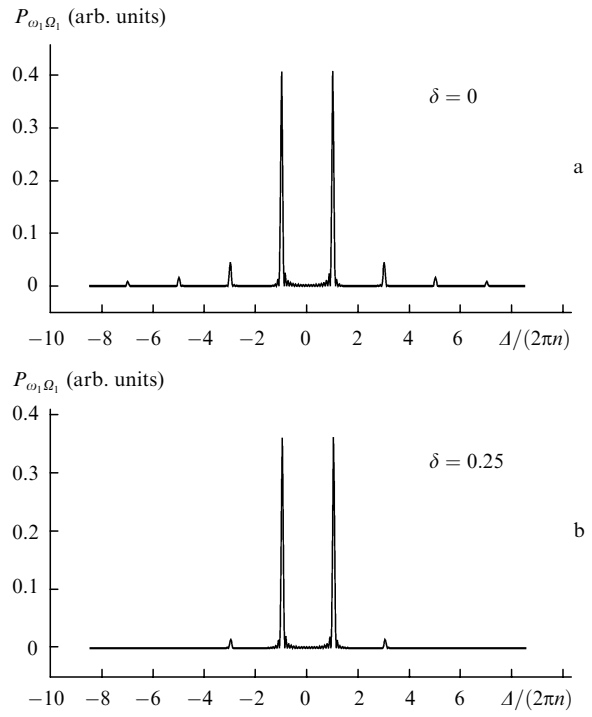

Figure 7. The SPS line shape in a transparent polydomain ferroelectric with domains of the same thickness, neglecting (a) and taking into account (b) intermediate layers between the domains.

($\delta \approx 0.25$). As the relative thickness of intermediate layers further increases, the spectrum acquires gradually the features that are typical for a sinusoidal distribution of $\chi^{(2)}$ corresponding to the limiting case $\delta = 0.5$. In this case, the middle regions of the homogeneous distribution of $\chi^{(2)}$ are absent, as well as scattering to any diffraction orders except the first ones.

The asymmetry of the spatial structure (unequal thicknesses of domains of opposite signs) is manifested in a qualitatively different way, leading to the violation of the unipolarity of the entire crystal. In this case, $|\rho| \neq 0$ and can achieve the value up to $1 - 2\delta$. Figure 8 shows the dependences of the differential power of signal radiation on the wave detuning for $\delta = 0$, $\rho = 0.25$, 0.5, 0.6, and 0.8. One can see that, as the domain asymmetry increases, first, the even orders of nonlinear diffraction appear and are relatively amplified. For the ratio of thicknesses of domains with opposites signs equal to 1 : 3 ($\rho = 0.5$), the central unshifted peak becomes greater than the rest of the peaks. As the difference in the domain thicknesses is further increased, the nonzero-order diffraction peaks become weaker and tend to levelling. The limiting values $\rho = \pm 1$ correspond to a monodomain crystal, and the shape of a parametric scattering line is described by the known dependence $\mathrm{sinc}^2(\Delta/2)$ with the main peak at the point $\Delta = 0$.

The presence of intermediate layers in asymmetric domain systems qualitatively affects the signal radiation spectra, as in the case of symmetric domains. As the relative thickness of the intermediate layer increases, the diffraction maxima with number $m = \pm 2$ and higher disappear. However, even the thickness of the middle layers of domains of any sign is zero and the value of ρ is maximal, the crystal does not become monodomain. The distribution of $\chi^{(2)}(z)$ and the shape of the signal radiation line for $l_2 = 0$ are

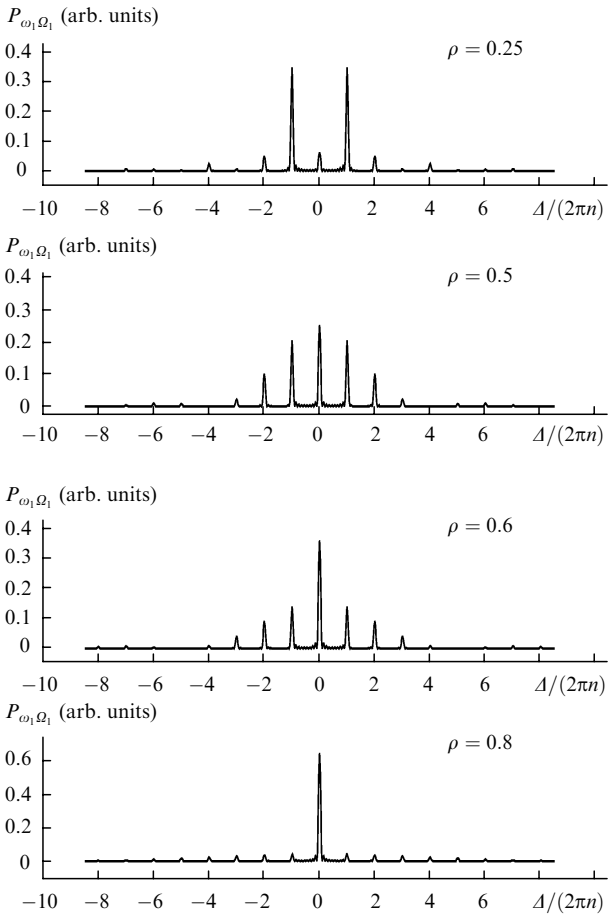

Figure 8. Effect of the domain asymmetry on the SPS line shape in a periodically poled transparent ferroelectric ($\delta = 0$).

shown in Fig. 9 ($\rho = 0.6$, $\delta = 0.2$). The characteristic feature of the distribution is the absence of nonlinear diffraction maxima with numbers $m = \pm 4$ and larger. The disappearance of the higher-order maxima in the signal radiation spectra points clearly to the presence of intermediate layers in the domain structure of the crystal.

The examples considered above illustrate qualitative conclusions following from general expressions for the intensities I_m of diffraction maxima of different orders. Indeed, in the general case of a periodic distribution of the quadratic susceptibility of type (6), the relations

$$I_m = (\bar{\chi}\rho)^2 \left[\frac{\cos(m\pi\delta)}{1-(2m\delta)^2}\right]^2 \times \begin{cases} \left[\dfrac{\sin(m\pi\rho/2)}{m\pi\rho/2}\right]^2, & \text{if } m \text{ is even}, \\ \left[\dfrac{\cos(m\pi\rho/2)}{m\pi\rho/2}\right]^2, & \text{if } m \text{ is odd} \end{cases} \tag{11}$$

follow from (8). Here, $I_m \equiv P_{\omega_1\Omega_1}\big|_{\Delta_m=0}/C_0$ are the differential powers of scattering measured in arbitrary units for $\Delta(\omega_1, \theta_1) = 2\pi mn$. One can see from (11) that the even orders of nonlinear diffraction are absent in unipolar domain systems with equal thicknesses of domains of opposite signs (i.e., for $\rho = 0$). The difference in the thicknesses of adjacent domains leads to scattering into

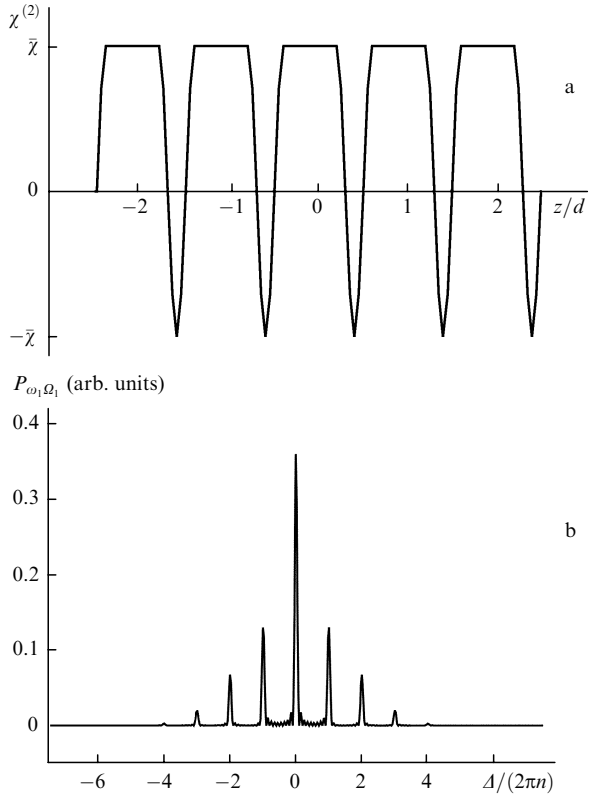

Figure 9. Distribution of the quadratic susceptibility $\chi^{(2)}(z)$ (a) and the SPS line shape in a ferroelectric with extremely thin domains of the same sign (b) ($\rho = 0.6$, $\delta = 0.2$).

even diffraction orders and the appearance of the unshifted tuning curve, which is typical for a monodomain crystal. In the presence of intermediate layers of a noticeable thickness (at the scale of the domain system period), the relation between the intensities of different peaks changes. When $m\pi\delta \ll 1$, the effect of intermediate layers leads to a simple decrease in the intensity of peaks of scattering into nonzero nonlinear diffraction orders:

$$I_m \approx \left(\frac{2\bar{\chi}}{\pi}\right)^2 \left(\frac{1}{m^2} - 1.87\delta^2\right) \times \begin{cases} \sin^2\dfrac{m\pi\rho}{2}, & \text{if } m \text{ is even,} \\ \cos^2\dfrac{m\pi\rho}{2}, & \text{if } m \text{ is odd.} \end{cases} \quad (12)$$

The above relations for peak intensities are also valid in many respects when the values of $\chi^{(2)}$ inside domains of opposite signs do not coincide. In this case, a constant component of the zero harmonic appears, which makes an additional contribution only to the zero-order maximum.

5. Diagnostics of the spatial distribution of $\chi^{(2)}$ by SPS spectra

Based on the results obtained in previous sections, we propose two schemes to analyse the frequency–angular distribution of the SPS intensity for determining the function $\chi^{(2)}(z)$ in an inhomogeneous structure with *a priori* unknown parameters. The first scheme is suitable for studying the parameters of regular 180° domain structures containing a great number of domains ($n \gg 1$), while the second one is convenient for determining the irregular distribution of $\chi^{(2)}(z)$ in systems containing a small number of domains ($n < 10$).

Extended regular domain structures are analysed by several stages using the first scheme.

The first stage. The individual tuning curves are fixed that are simultaneously observed in a two-dimensional frequency–angular scattering spectrum. The criterion is the observation of several (no less that two) maxima of comparable intensities upon scanning the frequency or scattering angle. The presence of several maxima points to nonlinear diffraction from a periodic structure. For a further consideration to be valid, the widths of the maxima should be substantially smaller than their separation. This condition can be not fulfilled when the resolution of a detector is not sufficient, when the periodicity of the domain system is strongly distorted, or in the case of strong absorption or a small number $2n$ of domains in a sample under study.

The second stage. The dependence of the differential power $P_{\omega_1\Omega_1}$ of SPS on the wave detuning $\Delta = \Delta(\omega_1, \theta_1)$ of phase matching is measured. Scanning can be performed in experiments over any combination of scattering angle–frequency parameters. Then, however, the scanning variable should be expressed in terms of phase detuning. This requires information on the dispersion of the refractive index of a crystal at the signal and idler frequencies, as well as at the pump frequency. Such *a priori* information for the idler frequencies is often absent. In this case, the phase mismatch at each scattering frequency can be determined only with an accuracy of a constant. The coordinate origin can be specified after the identification of the ordinal numbers m of diffraction maxima (see the next stage). Simultaneously, the refractive index of the crystal can be calculated at the idler wave frequency.

The third stage. The order of nonlinear diffraction corresponding to each maximum is determined. The identification of the diffraction order is based on the symmetry of the spectra: maxima with the numbers $+m$ and $-m$ should have the same intensity. The deviation fom the symmetry of the spectra points to the presence of blocks with different refractive indices in the crystal. The spectra of scattering into the lower orders of nonlinear diffraction should be equidistant. The deviation from the equidistance may point to the presence of several domain blocks with different periods in the region of the crystal involved in the formation of the SPS signal. By analysing the positions of symmetric equidistant maxima of the dependence $P_{\omega_1\Omega_1}(\Delta)$ in the frequency–scattering angle coordinates, one can find the position of the central maximum, which corresponds to the zero wave detuning Δ. Then, the lacking values of linear optical parameters of the crystal can be determined and the scale of the wave detunings Δ can be completely specified.

The fourth stage. The relation between the thicknesses of neighbouring domains is determined. If the scattering intensity at the centre of the distribution $P_{\omega_1\Omega_1}(\Delta)$ is zero, then the spectrum consists of only odd orders of nonlinear diffraction. This suggests that the thicknesses of domains of opposite signs are identical (the crystal is unipolar). The appearance of the nonzero-order maximum at the centre of the distribution $P_{\omega_1\Omega_1}(\Delta)$ (which has no symmetrically located analogue) suggests that the domains

of opposite signs have different thickness or the absolute values of $\chi^{(2)}$ in positive and negative domains are different.

The fifth stage. Depending on the results of the previous stage, two variants are possible:

Variant 1. Measurement of the parameters of a symmetric domain system (with equal thicknesses of domains of opposite signs). In this case, the spectrum exhibits the intense $\pm$1st-order maxima and substantially weaker maxima of higher odd orders, while the maxima of nonzero even orders are absent. The distance between the neighbouring odd maxima along the axis Δ is $4\pi l/(d\cos\theta)$. By measuring the frequency and angular shifts of maxima of different orders with respect to each other, the size $d/2$ of domains and their angle of inclination Δ to the entrance and exit faces of the crystal are determined. The larger is the width of the intermediate region at the domain boundary, the weaker are the higher-order maxima. The ratio of the intensities of the $\pm$1st- and $\pm$3rd-order maxima is

$$\frac{I_1}{I_3} = \left[\frac{3\cos(\pi\delta)}{\cos(3\pi\delta)}\,\frac{1-(6\delta)^2}{1-(2\delta)^2}\right]^2. \tag{13}$$

For $\delta \leqslant 0.1$, the ratio of the maxima is $I_1 : I_3 \simeq 10:1$. As the relative thickness δ of the intermediate layer increases, this ratio rapidly increases, achieving $\sim 100:1$ for $\delta \approx 0.36$ and $\sim 1000:1$ for $\delta \approx 0.45$. For $\delta \geqslant 0.4$, the SPS spectrum contains in fact only two tuning curves of scattering to the $\pm$1st diffraction orders, and the distribution $\chi^{(2)}(z)$ is identified as a sinusoidal one. In the intermediate cases, by approximating the ratio $I_1 : I_3$ by expression (11), we can find the thickness of the intermediate layer $2\Delta l \equiv \delta d$.

Variant 2. Measurement of the parameters of an asymmetric domain system (with unequal thicknesses of domains of opposite signs). In this case, the SPS spectrum contains maxima both of even and odd orders. The ratio of the $\pm$1st- and zero-order maxima is determined by the expression

$$\frac{I_1}{I_0} = \left[\frac{\cos(\pi\delta)}{1-(2\delta)^2}\,\frac{\cos(\pi\rho/2)}{\pi\rho/2}\right]^2, \tag{14}$$

which is valid when the absolute values of $\chi^{(2)}$ in the domains of opposite signs are identical; while the ratio of the $\pm$1st- and $\pm$2nd-order maxima is determined by the expression

$$\frac{I_1}{I_2} = \left[\frac{\cos(\pi\delta)}{\cos(2\pi\delta)}\,\frac{1-(4\delta)^2}{1-(2\delta)^2}\,\frac{1}{\sin(\pi\rho/2)}\right]^2. \tag{15}$$

Therefore, as the difference of the domain thicknesses increases, the relative weight of the first-order maxima rapidly decreases, whereas it increases with increasing the intermediate-layer thickness. The approximation of the measured ratios $I_1 : I_0$ and $I_1 : I_2$ by expressions (14) and (15) allows one to determine the values of δ and ρ, the thickness $2\Delta l$ of the intermediate layer, and the size of homogeneous regions in domains of opposite signs $l_1 \equiv d(1+\rho)/2$ and $l_2 \equiv d(1-\rho)/2$.

When $\chi^{(2)}(z)$ changes irregularly, the zero-order Fourier harmonics of the quadratic susceptibility determine the scattered power for $\Delta = 2\pi m$ ($m \neq 0$). It is for such values of the wave detuning that the differential power of SPS in a homogeneous medium $P_{\omega_1\Omega_1} = C_0[\chi\,\mathrm{sinc}\,(\Delta/2)]^2$ vanishes. The presence of a nonzero signal in a transparent medium, when the condition $\Delta = 2\pi m \neq 0$ is fulfilled, points to the inhomogeneous distribution of the quadratic susceptibility.

The second scheme for diagnostics of the profile of the spatially inhomogeneous distribution of $\chi^{(2)}(z)$ can be applied to analyse the structures containing a small number of domains of an arbitrary thickness. In this case, the overlap of nonlinear diffraction fringes of different orders can cause the shift of the intensity maxima from their positions corresponding to the quasi-phase-matching condition. This gives the possibility of measuring the amplitudes $|\chi_m|$ and phases φ_m of different harmonics of the quadratic susceptibility

$$\chi^{(2)}(z) = \sum_m |\chi_m| \exp[\mathrm{i}(2\pi m z + \varphi_m)].$$

The general scheme of the analysis can be divided into the following stages.

The first stage. The dependence of the differential SPS power $P_{\omega_1\Omega_1}$ on the wave detuning of phase matching $\Delta = \Delta(\omega_1, \theta_1)$ is measured. The measurements are performed in the same manner as at the initial stages of the first scheme.

The second stage. The ratio of the amplitudes $|\chi_m|$ is determined. For this purpose, the ratio of the intensities I_0 and I_m for the wave detuning $\Delta = 0$ and $2\pi m$, respectively, is measured. Then, the relative values $|\chi_m|/\chi_0 = (I_m/I_0)^{1/2}$ are calculated. If scattering in the unshifted direction is absent and $I_0 = 0$, the normalisation can be performed to any maximum of the nonzero intensity.

The third stage. The ratio of phases φ_m is determined by approximating the experimental dependence $P_{\omega_1\Omega_1}(\Delta)$ by the expression

$$\frac{P_{\omega_1\Omega_1}(\Delta)}{C_0\chi_0^2} = \mathrm{sinc}^2(\Delta/2)\left\{\left[\sum_{m=-\infty}^{\infty}\frac{(-1)^m|\chi_m|/\chi_0}{1-2\pi m/\Delta}\cos\varphi_m\right]^2 + \left[\sum_{m=-\infty}^{\infty}\frac{(-1)^m|\chi_m|/\chi_0}{1-2\pi m/\Delta}\sin\varphi_m\right]^2\right\} \tag{16}$$

successively on all intervals $2\pi m < \Delta < 2\pi(m+1)$ taking into account the measured relative amplitudes $|\chi_m|/\chi_0$ and the relation $\varphi_m = -\varphi_{-m}$.

The fourth stage. The profile of a variation in the quadratic susceptibility is calculated within the entire scattering volume by the expression

$$\frac{\chi^{(2)}(z)}{\chi_0} = \sum_m \frac{|\chi_m|}{\chi_0}\exp[\mathrm{i}(2\pi m z + \varphi_m)].$$

6. Effect of absorption on the shape of an SPS line in nonlinear periodic structures

The presence of absorption only at the idler frequency or at the signal and idler frequencies leads to a significant change in the spectral and angular distributions of the signal intensity. This should be taken into account in the diagnostics of the spatial distribution of the quadratic susceptibility and in calculations of the parameters of parametric devices based on quasi-phase-matched converters and optical oscillators.

If the spectrum of the spatial harmonics of the quadratic susceptibility is known, the shape of the SPS line in the case

of absorption can be calculated by the expression

$$P_{\omega_1\Omega_1} = 2C_0\{(e^{-y_2}\cos\Delta - 1)[(y_2^2 - \Delta^2)Z'(y_2,\Delta) - Z''(y_2,\Delta) + (2y_2\Delta)^2 X'(y_2,\Delta)] + 2e^{-y_2}y_2\Delta\sin\Delta \times [Z'(y_2,\Delta) - (y_2^2 - \Delta^2)X'(y_2,\Delta) + X''(y_2,\Delta)] + y_2 G(y_2,\Delta)\}, \quad (17)$$

which follows directly from (1). Here,

$$Z'^{(\prime\prime)}(y_2,\Delta) \equiv [W'^{(\prime\prime)}(y_2,\Delta)]^2 - [2y_2\Delta u'^{(\prime\prime)}(y_2,\Delta)]^2,$$

$$X'^{(\prime\prime)}(y_2,\Delta) \equiv 2u'^{(\prime\prime)}(y_2,\Delta)W'^{(\prime\prime)}(y_2,\Delta),$$

$$W'^{(\prime\prime)}(y_2,\Delta) \equiv (y_2^2 - \Delta^2)u'^{(\prime\prime)}(y_2,\Delta) + v'^{(\prime\prime)}(y_2,\Delta),$$

$$u'(y_2,\Delta) \equiv \sum_{m=-\infty}^{\infty} \frac{(-1)^m \chi'_m}{\varphi_m(y_2,\Delta)},$$

$$u''(y_2,\Delta) \equiv \sum_{m=-\infty}^{\infty} \frac{(-1)^m \chi''_m}{\varphi_m(y_2,\Delta)} 2\pi mn, \quad (18)$$

$$v'(y_2,\Delta) \equiv \sum_{m=-\infty}^{\infty} \frac{(-1)^m \chi'_m}{\varphi_m(y_2,\Delta)} (2\pi mn)^2,$$

$$v''(y_2,\Delta) \equiv \sum_{m=-\infty}^{\infty} \frac{(-1)^m \chi''_m}{\varphi_m(y_2,\Delta)} (2\pi mn)^3,$$

$$\varphi_m(y_2,\Delta) \equiv (y_2^2 + \Delta^2)^2 + 2(y_2^2 - \Delta^2)(2\pi mn)^2 + (2\pi mn)^4,$$

$$G(y_2,\Delta) \equiv \sum_{m=-\infty}^{\infty} \frac{|\chi'_m|^2 + |\chi''_m|^2}{y_2^2 + (\Delta - 2\pi mn)^2}, \quad \chi_m \equiv \chi'_m + i\chi''_m.$$

Consider the shape of the SPS line for a few particular nonlinear structures with nonzero absorption at the idler frequency. For regular polydomain crystals with equal thicknesses of domains of opposites signs and the meander distribution of the nonlinear susceptibility, the exact calculation by expression (17) gives the dependence

$$P_{\omega_1\Omega_1} = 2C_0 \frac{\bar{\chi}^2}{y_2^2 + \Delta^2}\left\{(e^{-y_2}\cos\Delta - 1)\left[\frac{y_2^2 - \Delta^2}{y_2^2 + \Delta^2} \times \frac{\sin^2\Delta'' - \sinh^2 y_2''}{(\cosh y_2'' + \cos\Delta'')^2} - 4\frac{y_2\Delta}{y_2^2 + \Delta^2}\frac{\sinh y_2''\sin\Delta''}{(\cosh y_2'' + \cos\Delta'')^2}\right] - 2e^{-y_2}\sin\Delta\left[\frac{y_2\Delta}{y_2^2 + \Delta^2}\frac{\sin^2\Delta'' - \sinh^2 y_2''}{(\cosh y_2'' + \cos\Delta'')^2} + \frac{y_2^2 - \Delta^2}{y_2^2 + \Delta^2}\frac{\sinh y_2''\sin\Delta''}{(\cosh y_2'' + \cos\Delta'')^2}\right] + y_2 - 4n\left[\frac{y_2^2 - \Delta^2}{y_2^2 + \Delta^2} \times \frac{\sinh y_2''}{\cosh y_2'' + \cos\Delta''} + 2\frac{y_2\Delta}{y_2^2 + \Delta^2}\frac{\sin\Delta''}{\cosh y_2'' + \cos\Delta''}\right]\right\}. \quad (19)$$

Here,

$$y_2'' \equiv \frac{\alpha_2(d/2)}{2\cos\vartheta_2}, \quad \Delta'' \equiv \frac{d}{2}(|k_{1z}| + |k_{2z}| - |k_{0z}|)$$

is the absorption of the idler wave and the wave detuning over the domain length $d/2$, respectively. This power distribution describes nonlinear diffraction to odd orders. The presence of absorption at the idler frequency results in the broadening of each diffraction maximum without its shift (Fig. 10).

As a rule, the thickness of PPCs is rather large and they contain a great number of periods $n \equiv l/d$. In a broad spectral range, the case can be realised when absorption in one domain is very weak, while the crystal as a whole is opaque for idler waves: $y_2/n \sim 1$, $y_2 \gg 1$, $n \gg 1$. For domains of thickness 1–10 μm, these relations are satisfied, for example, in the polariton part of the spectrum, when α_2 achieves the value of the order of 10^3 cm^{-1} and above. If the

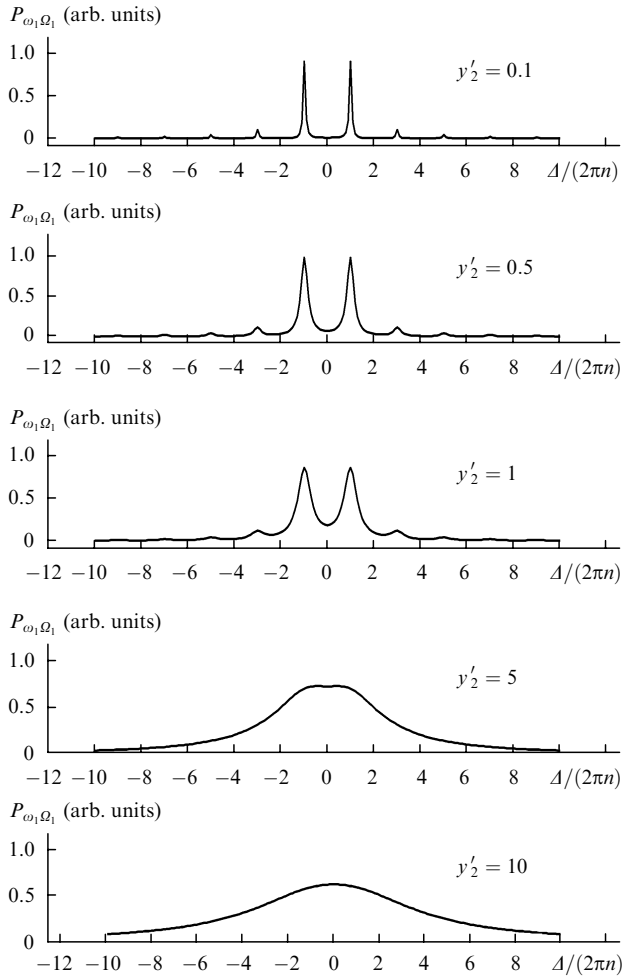

Figure 10. Effect of absorption on the SPS line shape in ferroelectrics with a symmetric regular domain structure (calculation performed for $n = 10$).

number of domains in this case is sufficiently large ($n \gg 1$) and $n \gg y_2/n$, the expression

$$P_{\omega_1\Omega_1} = 2C_0 y_2 \sum_{m=-\infty}^{\infty} \frac{|\chi_m|^2}{y_2^2 + (\Delta - 2\pi mn)^2} \tag{20}$$

follows from (1) for any distribution of the quadratic susceptibility. The width of each nonlinear diffraction peak in the scale Δ is determined by absorption y_2 over the entire length $l = nd$ of the crystal. The diffraction structure is observed if absorption over one period length $y_2' \equiv y_2/n$ remains weak. In this case, information on the phases of complex amplitudes χ_m is lost. However, the ratio of amplitudes $|\chi_m|$ can be determined from the ratio of diffraction maxima. If absorption y_2' over one period length is large, i.e., $y_2' \gg 1$, the nonlinear diffraction bands almost completely merge, and the minima of the diffraction pattern become indistinguishable. The parametric scattering line is described by a broad Lorentzian with a maximum at the point $\Delta = 0$.

$$P_{\omega_1\Omega_1} \sim \frac{y_2}{y_2^2 + \Delta^2}. \tag{21}$$

In this case, as for a homogeneous monodomain crystal, the half-width of the scattering line is determined by absorption y_2 in the crystal. The influence of the number of domains on the shape of the SPS line ($y_2' = 2$) is illustrated in Fig. 11. As the number of domain periods increases from 1 to 10, the diffraction structure of the line becomes more distinct if absorption in one domain is weak and the diffraction structure is still visible. A further increase in the number of domains almost does not affect the visibility of the diffraction pattern. If absorption is strong ($y_2' \geqslant 10$), a satisfactory visibility cannot be obtained by increasing the number of domains.

In nonlinear interferometers representing structures assembled from alternating layers of optically nonlinear ($\chi^{(2)} \neq 0$) and optically linear materials, the GKL method allows one to take into account possible absorption both in linear and nonlinear layers. The relations obtained in previous sections are valid when the real and imaginary parts of the dielectric constant of the layers weakly differ from each other. Structures consisting of alternating optically linear and nonlinear layers with the homogeneous distribution of the linear susceptibility can be assembled from successively arranged plane–parallel plates cut from the same nonlinear crystal but at different angles to its crystallographic axes. If the thickness of the plates is the same, the distribution of the signal power is described by the expression

$$P_{\omega_1\Omega_1} = 4C_0 \frac{\bar{\chi}^2}{y_2^2 + \Delta^2} \left\{ \left(e^{-y_2}\cos\Delta - 1\right) \left[\frac{y_2^2 - \Delta^2}{y_2^2 + \Delta^2} \times \right.\right.$$

$$\times \frac{1 + \cosh y_2'' \cos\Delta''}{(\cosh y_2'' + \cos\Delta'')^2} - \frac{2y_2\Delta}{y_2^2 + \Delta^2} \frac{\sinh y_2'' \sin\Delta''}{(\cosh y_2'' + \cos\Delta'')^2} \Bigg]$$

$$- e^{-y_2} \sin\Delta \left[\frac{2y_2\Delta}{y_2^2 + \Delta^2} \frac{1 + \cosh y_2'' \cos\Delta_2'}{(\cosh y_2'' + \cos\Delta'')^2} \right.$$

$$\left. + \frac{y_2^2 - \Delta^2}{y_2^2 + \Delta^2} \frac{\sinh y_2'' \sin\Delta''}{(\cosh y_2'' + \cos\Delta'')^2} \right] + y_2 - 2n \left[\frac{y_2^2 - \Delta^2}{y_2^2 + \Delta^2} \right.$$

$$\left.\left. \times \frac{\sinh y_2''}{\cosh y_2'' + \cos\Delta''} + 2\frac{y_2\Delta}{y_2^2 + \Delta^2} \frac{\sin\Delta''}{\cosh y_2'' + \cos\Delta''} \right] \right\}. \tag{22}$$

Here, $\bar{\chi}$ is the quadratic susceptibility of an optically nonlinear layer. Figure 12 shows the examples of scattering lines, which are typical for symmetric and extremely asymmetric interferometers ($n = 10$, $y_2' = 1$). In the case of maximum values of $\rho > 0$, when the thickness l_1 of nonlinear layers is substantially greater than the thickness l_2 of linear layers, the shape of the line is close to the power distribution in a homogeneous nonlinear layer with the same total thickness. In the opposite situation, when the thickness of nonlinear layers is extremely small ($\rho < 0$), the spectrum consists of very weak equidistant nonlinear diffraction maxima.

In polydomain regular crystals, thin optically nonlinear layers can appear near domain boundaries due to a change in the mutual orientation of crystallographic axes upon passing from one domain to another, even when $\chi^{(2)} = 0$ inside each domain. In this case, when the thickness of domains is the same, the periodic distribution of $\chi^{(2)}(z)$ will be described by alternating layers of thickness l_1 with the susceptibility $\chi^{(2)} = \bar{\chi} \neq 0$ (intermediate layers) and of thickness l_2 with $\chi^{(2)} = 0$ (domains). When the thicknesses of linear and nonlinear layers differ significantly ($x \equiv l_1/d \ll 1$), the signal intensity can be calculated assuming that $\chi_m \approx 2x(-1)^{mn}\bar{\chi}$. For an odd number n of domains, the shape of the SPS line will be determined by the expression

$$P_{\omega_1\Omega_1} = \frac{C_0 (l_1/l)^2 \bar{\chi}^2 n}{\cosh y_2' - \cos\Delta'} \left\{ 4\sinh y_2' + \frac{1}{2n(\cosh y_2' - \cos\Delta')} \right.$$

$$\times \left[\left(e^{-y_2}\cos\Delta - 1\right)\left(\sinh^2 y_2' - \sin^2\Delta'\right) + \right.$$

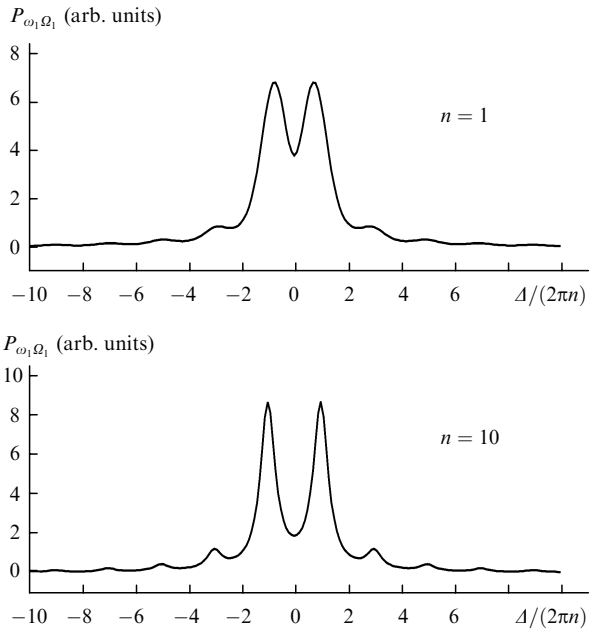

Figure 11. Effect of the number of domains of the SPS line shape in a polydomain crystal absorbing idler radiation ($y_2' = 2$, $\rho = \delta = 0$).

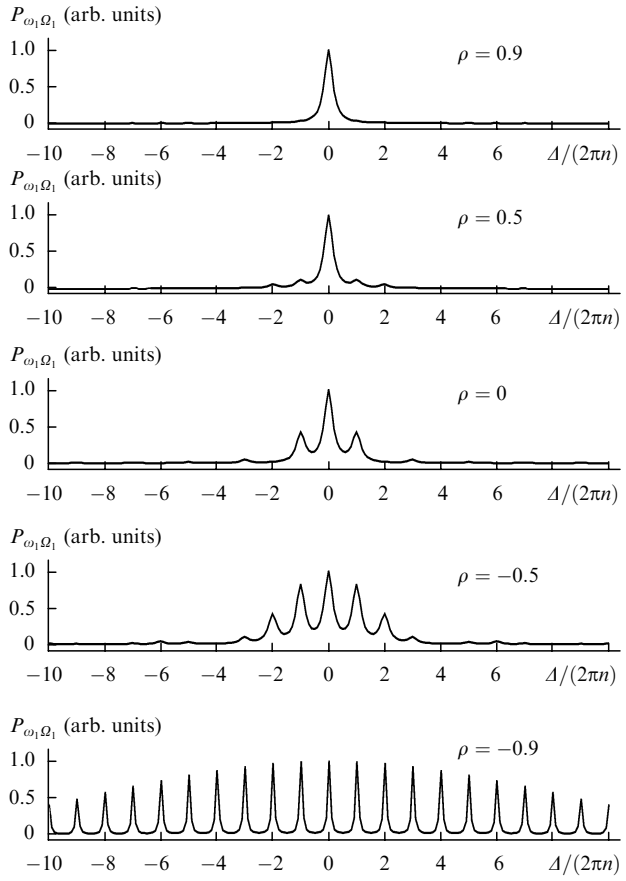

Figure 12. Effect of the ratio of thicknesses of linear and nonlinear layers on the SPS line shape in a nonlinear interferometer ($n = 10$, $y_2' = 1$).

$$+ 2e^{-y_2} \sin\Delta \sin\Delta' \sinh y_2'\Big]\Big\}. \qquad (23)$$

Here, Δ' is the phase mismatch over one period length. The total signal intensity is determined by the interference of signals from individual nonlinear layers. As a result, the intensity distribution consists of equidistant diffraction maxima. As in a homogeneous crystal, the stronger is absorption, the larger is the width of each scattering line. In the approximation of thin nonlinear layers ($l_1/d \ll 1$), the intensity of the diffraction maxima slowly decreases with increasing diffraction order.

7. Conclusions

We have obtained general expressions and considered different particular cases of the distribution of the differential SPS power in spatially inhomogeneous layered media. A direct relation has been established between the shape of the signal line (the dependence of the SPS power on the wave detuning) and the spatial Fourier spectrum of the quadratic susceptibility of the medium. In an optically transparent medium, this relation is the same for all the three types of three-wave processes, both spontaneous and simulated, both for the frequency summation and subtraction. Absorption at the frequencies of all the three waves involved in SPS affects differently the shape of the signal line. Because the influence of absorption at the idler-wave frequencies is most interesting for applications, we have considered effects caused by this absorption.

The dependence of the shape of the SPS line on the spatial distribution of the quadratic susceptibility can be used for tomography of the spatial distribution of $\chi^{(2)}$ in polydomain crystals, nonlinear interferometers, and other structures where the effective value of $\chi^{(2)}$ substantially varies in the volume. We have presented algorithms for diagnostics of one-dimensional nonlinear superlattices in PPCs and schemes for measuring irregular distributions of $\chi^{(2)}$ in relatively thin layers with variable $\chi^{(2)}$. Each diagnostic scheme can be used not only to determine the PPC period and orientation but also to reconstruct the profile of variation in $\chi^{(2)}$ over the PPC period or over an irregular inhomogeneous layer. Note that all these measurements are non-destructive and characterise the distribution of $\chi^{(2)}$ over the entire volume of a sample contributing to a nonlinear signal. The proposed methods can be also used for diagnostics of three-dimensional inhomogeneities of $\chi^{(2)}$ (it seems that possible complications of the schemes will be only of a technical type).

The relations obtained in the paper can be used for diagnostics of transparent inhomogeneous nonlinear media by the shape of not only the SPS line but also of signals of any stimulated three-wave parametric process. Due to their greater intensity, stimulated processes are preferable for analysis of irregular distributions of $\chi^{(2)}$ in thin layers in nonlinear interferometers. However, the obvious advantage of spontaneous scattering is that the SPS diagnostics does not require any additional incident idler radiation, and the signal spectrum is very broad and is determined only by the spatial inhomogeneity of a nonlinear medium and by the known spectrum of zero fluctuations of vacuum.

In the case of the stimulated process, the external idler radiation is required, and the shape of the signal line depends not only on the spatial distribution of $\chi^{(2)}$ but also on the distribution of brightness among the idler-radiation modes. As a rule, a high-power signal is obtained using idler radiation from lasers, which nonuniformly fills a narrow spectrum of the idler modes. The dependence of the signal intensity on the phase mismatch is determined by scanning the frequency or the angle of incidence of external radiation on a crystal. This complicates the method and requires the collection of a signal from the same region of a spatially inhomogeneous medium after each variation in the parameters of external radiation. In contrast to this, the shape of the SPS signal is always measured for the same region of a medium when the idler modes are filled uniformly.

Acknowledgements. This work was supported by the Russian Foundation for Basic Research (Grant No. 03-02-16364) and by Grant No. NSh-166.2003.02 for the Support of Leading Scientific Schools of RF.

References

1. Byer R.L. *Nonlinear Optics*, **7**, 235 (1994); Byer R.L. *J. Nonlinear Optical Physics & Materials*, **6**, 549 (1997).
2. Lu Y., Mao L., Ming N. *Opt. Lett.*, **19**, 1037 (1994).
3. Myers L.E., Miller G.D., Eckardt R.C., Fejer M.M., Byer R.L. *Opt. Lett.*, **20**, 52 (1995).

4. Aleksandrovskii A.L. *Vestn. Mosk. Univ., Ser. III*, **22**, 51 (1981); Aleksandrovskii A.L., Volkov V.V. *Kvantovaya Elektron.*, **23**, 557 (1996) [*Quantum Electron.*, **26**, 542 (1996)].
5. Bokhin A.V., Dmitriev V.G. *Kvantovaya Elektron.*, **32**, 219 (2002) [*Quantum Electron.*, **32**, 219 (2002)].
6. Chen D.-W. *J. Opt. Soc. Am. B*, **20**, 1527 (2003).
7. Chirkin A.S., Volkov V.V., Laptev G.D., Morozov E.Yu. *Kvantovaya Elektron.*, **30**, 847 (2000) [*Quantum Electron.*, **30**, 847 (2000)].
8. Kravtsov N.V., Laptev G.D., Naumova I.I., Novikov A.A., Firsov V.V., Chirkin A.S. *Kvantovaya Elektron.*, **32**, 923 (2002) [*Quantum Electron.*, **32**, 923 (2002)].
9. Kitaeva G.Kh., Mikhailovskii A.A., Penin A.N. *Zh. Eksp. Teor. Fiz.*, **112**, 2001 (1997).
10. Vidakovič P., Lovering D.J., Levenson J.A. *Opt. Lett.*, **22**, 277 (1997).
11. Asobe M., Yokohama I., Itoh H., Kaino T. *Opt. Lett.*, **22**, 274 (1997).
12. Serkland D.K., Fejer M.M., Byer R.L., Yamamoto Y. *Opt. Lett.*, **20**, 1649 (1995).
13. Chirkin A.S. *J. Opt. B*, **4**, S91 (2002).
14. Tanzilli S., De Riedmatten H., Tittel W., Zbinden H., Baldi P., De Micheli M., Ostrowsky D.B., Gisin N. *Electron. Lett.*, **37**, 26 (2001); *European Physical J. D*, **18**, 155 (2002).
15. Yablonovitch E. *J. Phys.: Condens. Matter*, **5**, 2343 (1993).
16. *J. Opt. Soc. Am. B*, Special Issue, **10**, 279–413 (1993).
17. D'Aguanno G., Centini M., Scalora M., Sibilia C., Dumeige Y., Vidakovič P., Levenson J.A., Bloemer M.J., Bowden C.M., Haus J.W., Bertolotti M. *Phys. Rev. E*, **64**, 016609 (2001).
18. Konotop V., Kuzmiak V. *Phys. Rev. B*, **66**, 235208 (2002).
19. Haus J.W., Viswanathan R., Scalora M., Kalocsai A.G., Cole J.D., Theimer J. *Phys. Rev. A*, **57**, 2120 (1998).
20. Balakin A.V., Bushuev V.A., Mantsyzov B.I., Ozheredov I.A., Petrov E.V., Shkurinov A.P. *Phys. Rev. E*, **63**, 046609 (2001).
21. Dumeige Y., Sagnes I., Mounier P., Vidakovič P., Abram I., Meriadec C., Levenson J.A. *Phys. Rev. Lett.*, **89**, 043901 (2002).
22. Dolgova T.V., Maidukovski A.I., Martemyanov M.G., Feduanin A.A., Aksipetrov O.A., Marowsky G., Yakovlev V.A., Mattei G., Ohta N., Nakabayashi S. *J. Opt. Soc. Am. B*, **19**, 2129 (2002).
23. Zhu S.N., Zhu Y.Y., Qin Y.Q., Wang H.F., Ge C.Z., Ming N.B. *Phys. Rev. Lett.*, **78**, 2752 (1997); Qin Y.Q., Su H., Tang S.H. *Appl. Phys. Lett.*, **83**, 1071 (2003).
24. Uesu Y., Kurimura S., Yamamoto Y. *Appl. Phys. Lett.*, **66**, 2165 (1995).
25. Cudney R.S., Garces-Chavez V., Negrete-Regagnon P. *Opt. Lett.*, **22**, 439 (1997).
26. Bloembergen N. USA patent 3 384433 (1968); Armstrong J., Bloembergen N., Ducuing J., Pershan P.S. *Phys. Rev.*, **127**, 1918 (1962); Bloembergen N., Sievers A.J. *Appl. Phys. Lett.*, **17**, 483 (1970).
27. Van der Ziel J.P., Bloembergen N. *Phys. Rev.*, **135**, A1662 (1964).
28. Chirkin A.S., in *Nelineinaya optika* (Nonlinea Optics) (Novosibirsk: Nauka, 1968) p. 202.
29. Miller R.C. *Phys. Rev.*, **134**, A1313 (1964).
30. Golenishchev-Kutuzov A.V., Golenishchev-Kutuzov V.A., Kalimullin R.I. *Usp. Fiz. Nauk*, **170**, 697 (2000).
31. Bryan D.A., Gerson R., Tomaschke H.E. *Appl. Phys. Lett.*, **44**, 847 (1984).
32. Volk T., Wohlecke M., Rubinina N., Reichert A., Razumovsky N. *Ferroelectrics*, **183**, 291 (1996).
33. Magel G.A., Fejer M.M., Byer R.L. *Appl. Phys. Lett.*, **56**, 108 (1990).
34. Fejer M.M., Magel G.A., Jundt D.H., Byer R.L. *IEEE J. Quantum Electron.*, **28**, 2631 (1992).
35. Ito H., Takyu C., Inaba H. *Electron. Lett.*, **27**, 1221 (1991).
36. He J., Tang S.H., Qin Y.Q., Dong P., Zhang H.Z., Kang C.H., Sun W.X., Shen Z.X. *J. Appl. Phys.*, **93**, 9943 (2003).
37. Lu Y., Xue C., Ming N. *Appl. Phys. Lett.*, **68**, 1467 (1996).
38. Naumova I.I., Gliko O.A. *Kristallographia*, **41**, 1 (1996).
39. Evlanova N.F., Naumova I.I., Chaplina T.O., Lavrishchev S.V., Blokhin S.A. *Fiz. Tverd. Tela*, **42**, 1678 (2000).
40. Naumova I.I., Evlanova N.F., Gliko O.A., Lavrishchev S.V. *J. Cryst. Growth*, **180**, 160 (1997).
41. Aleksandrovskii A.L., Gliko O.A., Naumova I.I., Pryalkin V.I. *Kvantovaya Elektron.*, **23**, 657 (1996) [*Quantum Electron.*, **26**, 641 (1996)].
42. Freund I. *Phys. Rev. Lett.*, **21**, 1404 (1968).
43. Grechin S.G., Dmitriev I.G., Yur'ev Yu.V. *Kvantovaya Elektron.*, **26**, 155 (1999) [*Quantum Electron.*, **29**, 155 (1999)].
44. Grechin S.G., Dmitriev I.G. *Kvantovaya Elektron.*, **26**, 151 (1999) [*Quantum Electron.*, **29**, 151 (1999)].
45. Grilli S., Ferraro P., De Nicola S., Finizio A., Pierattini G., De Natale P., Chiarini M. *Optics Express*, **11**, 392 (2003).
46. Holmgren S.J., Pasiskevicius V., Wang S., Laurell F. *Opt. Lett.*, **28**, 1555 (2003).
47. Klyshko D.N. *Fotony i nelineinaya optika* (Photons and Nonlinear Optics (Moscow: Nauka, 1980).
48. Klyshko D.N. *Usp. Fiz. Nauk*, **164**, 1187 (1994).
49. Mandel L. *Rev. Mod. Phys.*, **71**, S274 (1999).
50. Zeilinger A. *Rev. Mod. Phys.*, **71**, S288 (1999).
51. Klyshko D.N., Kutsov V.F., Penin A.N., Polkovnikov B.F. *Zh. Eksp. Teor. Fiz.*, **62**, 1291 (1972).
52. Polivanov Yu.N. *Usp. Fiz. Nauk*, **126**, 185 (1978).
53. Mavrin B.N., Sterin Kh.E. *Pis'ma Zh. Eksp. Teor. Fiz.*, **16**, 265 (1972).
54. Kitaeva G.Kh., Kuznetsov K.A., Naumova I.I., Penin A.N. *Kvantovaya Elektron.*, **30**, 726 (2000) [*Quantum Electron.*, **30**, 726 (2000)].
55. Klyshko D.N. *Kvantovaya Elektron.*, **4**, 1056 (1977) [*Sov. J. Quantum Electron.*, **7**, 591 (1977)].
56. Klyshko D.N. *Kvantovaya Elektron.*, **7**, 1932 (1980) [*Sov. J. Quantum Electron.*, **10**, 1112 (1980)].
57. Klyshko D.N., Penin A.N. *Usp. Fiz. Nauk*, **152**, 653 (1987).
58. Abroskina O.A., Kitaeva G.Kh., Penin A.N. *Dokl. Akad. Nauk SSSR*, **280**, 584 (1985).
59. Penin A.N., Sergienko A.V. *Appl. Opt.*, **30**, 3582 (1991).
60. Klyshko D.N. *Zh. Eksp. Teor. Fiz.*, **104**, 2676 (1993).
61. Burlakov A.V., Kulik S.P., Penin A.N., Chekhova M.V. *Zh. Eksp. Teor. Fiz.*, **113**, 1991 (1998).
62. Korystov D.Yu., Kulik S.P., Penin A.N. *Kvantovaya Elektron.*, **30**, 921 (2000) [*Quantum Electron.*, **30**, 921 (2000)].
63. Korystov D.Yu., Kulik S.P., Penin A.N. *Pis'ma Zh. Eksp. Teor. Fiz.*, **73**, 248 (2001).
64. Burlakov A.V., Mamaeva Yu.B., Penin A.N., Chekhova M.V. *Zh. Eksp. Teor. Fiz.*, **120**, 67 (2001).
65. Klyshko D.N. *Izv. Akad. Nauk SSSR, Ser. Fiz.*, **46**, 1478 (1982).
66. Kitaeva G.Kh., Penin A.N. *Zh. Eksp. Teor. Fiz.*, **125**, 307 (2004).
67. Klyshko D.N. *Zh. Eksp. Teor. Fiz.*, **55**, 1006 (1968).
68. Kitaeva G.Kh., Klyshko D.N., Taubin I.V. *Kvantovaya Elektron.*, **9**, 561 (1982) [*Sov. J. Quantum Electron.*, **12**, 333 (1982)].

69. Shen Y.R. *The Principles of Nonlinear Optics* (New York: John Wiley & Sons, 1984; Moscow: Nauka, 1989).
70. Akhmanov S.A., Khokhlov R.V. *Problemy nelineinoi optiki* (Problems of Nonlinear Optics) (Moscow: Izd. Akad. Nauk SSSR, 1965).
71. Scalora M., Bloemer M.J., Manka A.S., Dowling J.P., Bowden C.M., Viswanathan R., Haus J.W. *Phys. Rev. A*, **56**, 3166 (1997).
72. Steel M.J., Martijn de Sterke C. *Appl. Opt.*, **35**, 3211 (1996).
73. Martijn de Sterke C., Sipe J.E. *Phys. Rev. A*, **38**, 5149 (1988).
74. Aleksandrovskii A.L., Leont'eva I.N., Naumova I.I. *Vestn. Mosk. Univ., Ser. III*, **20**, 30 (1979).
75. Aleksandrovskii A.L., Maskaev Yu.A., Naumova I.I. *Fiz. Tverd. Tela*, **17**, 3192 (1975).
76. Naumova I.I., Evlanova N.F., Lavrishchev S.V., Blokhin S.A., Chaplina T.O., Chernevich T.G., Shustin O.A. *Mater. Elektron. Tekhn.*, (1), 30 (1999).
77. Kitaeva G.Kh., Kulik S.P., Penin A.N., Chekhova M.V. *Proc. SPIE Int. Soc. Opt. Eng.*, **1863**, 192 (1993).
78. Aleksandrovskii A.L., Kitaeva G.Kh., Kulik S.P., Penin A.N. *Zh. Eksp. Teor. Fiz.*, **90**, 1051 (1986).
79. Kitaeva G.Kh., Kulik S.P., Penin A.N. *Fiz. Tverd. Tela*, **34**, 3440 (1992).
80. Kitaeva G.Kh., Mikhailovsky A.A., Naumova I.I., Losevsky P.S., Penin A.N. *Appl. Phys. B*, **66**, 201 (1998).